

Solar Panel Efficiency Enhancement through Water Cooling with IoT Integration

Adam BimaJaya*, Agustian Damar Permana, Hedy Devitra

Department of Electrical Engineering, Universitas Maritim Raja Ali Haji, Tanjung Pinang, Indonesia

*Correspondence: 2101010025@student.umrah.id

<https://doi.org/10.62777/pec.v2i1.53>

Received: 11 March 2025

Revised: 8 April 2025

Accepted: 16 April 2025

Published: 1 May 2025



Copyright: (c) 2025 by the authors.
This work is licensed under a
Creative Commons Attribution 4.0
International License.

Abstract: The efficiency of photovoltaic (PV) solar panels declines significantly with increasing temperature due to the thermal sensitivity of semiconductor materials. To mitigate this issue, various cooling strategies—particularly water-based systems—have been explored. This study presents the design and implementation of an Internet of Things (IoT)-based monitoring system to assess the impact of water cooling on PV panel performance. Experiments were conducted in a laboratory environment using observational methods, with data collected at 30-second intervals and visualized via the ThingSpeak platform. Results show that panels equipped with water cooling maintained lower operating temperatures and generated higher average voltage outputs than non-cooled counterparts. These findings confirm a positive correlation between temperature reduction and enhanced panel efficiency. While current measurements were not directly analyzed due to the system's solar charge controller (SCC) configuration, the overall setup proved effective for real-time performance monitoring and demonstrates the potential of IoT integration in optimizing solar energy systems, particularly for large-scale applications.

Keywords: Solar panel, water cooling, efficiency, IoT, ThingSpeak

1. Introduction

The growing need for sustainable energy solutions has prompted a global shift toward renewable sources. Among them, solar energy stands out for its abundance availability [1]. However, one of the key challenges in optimizing the performance of solar panels lies in their susceptibility to temperature increases [2]. The efficiency of photovoltaic panels decreases as the panel temperature rises, due to the temperature-sensitive nature of semiconductor materials, which impairs the flow of electrons and reduces voltage output [3], [4], [5], [6].

Studies have shown that solar panels without temperature regulation can experience a noticeable drop in efficiency [7]. To address this issue, various cooling techniques have been explored, ranging from passive solutions to active cooling methods [8]. For instance, Chanpavong *et al.* showed that an active cooling system using water circulation improved solar panel efficiency by up to 12.76% compared to panels without cooling [9].

To maintain optimal performance, continuous monitoring of solar panel parameters such as temperature, voltage, and current is essential. Manual monitoring,

however, is impractical for large scale solar installations. This is where the Internet of Things (IoT) offers a compelling solution. By integrating IoT into solar panel systems, it becomes possible to automate data collection and remotely supervise performance in real time [10]. This research proposes the development of an IoT-based monitoring system designed to track the operational conditions of solar panels, with a focus on temperature induced efficiency loss. Such a system is particularly beneficial in large scale solar farms, where centralized oversight is essential for efficient energy production.

2. Materials and Methods

2.1. System Components

This study employed a variety of electronic components to develop an IoT-based monitoring system for evaluating the influence of water cooling on photovoltaic (PV) panel efficiency. The main hardware components are as follows:

- **NodeMCU ESP32 module:** The NodeMCU is a development tool utilizing the ESP32, capable of connecting to both Wi-Fi and Bluetooth. NodeMCU is an open-source software that can be programmed via the Arduino IDE.
- **RTC DS3231 Module:** The RTC module is an electronic component capable of providing information on hours, minutes, and seconds, as well as details about the date and year through I2C communication [11]. The RTC (Real-Time Clock) module is also equipped with a 3V battery to maintain functionality when the main power source is unavailable.
- **SD Card Adapter Module:** The SD Card Adapter module enables reading SD cards through SPI communication and can function as offline data storage [12]. Although data can be stored online via the Thingspeak server, which is used as the IoT platform, this module is required as a backup for offline data storage.
- **INA219 Sensor:** The INA219 sensor is a module used to measure both voltage and current in an electrical circuit. The INA219 sensor can connect to various devices through I2C communication. This sensor is capable of measuring currents up to 3.2 A and detecting voltages ranging from 0 to 26 Vdc [13]. Previous research showed that the INA219 sensor has an accuracy of 99.96% for voltage and 98.39% for current [14].
- **DS18B20 Sensor:** The DS18B20 sensor is an electronic device capable of detecting temperature changes and converting them into electrical quantities. This digital sensor connects through one-wire communication. Its unique feature is that each DS18B20 sensor has a serial code, allowing multiple DS18B20 sensors to be used on a single one-wire communication line [15]. Previous research has shown that the DS18B20 sensor has a measurement accuracy of 99.05%, higher than the DHT22 (98.15%) and DHT11 (97.19%) [16].
- **Solar Charge Controller:** The Solar Charge Controller (SCC) is a crucial component in photovoltaic systems, serving to regulate the electrical current from the solar panel to the battery and load. The SCC also acts as a safeguard to prevent the battery from overcharging [17].
- **DC Lamp:** Direct current lamp is a light source that operates using a DC power supply. The DC lamp is utilized as a load in this circuit.
- **Solar Panel:** A solar panel is a collection of several solar cells that convert solar energy into electrical energy through the photovoltaic process [18].
- **Lead-acid battery:** The battery is used as a power storage device for the energy generated by the solar panel.

- **DC water pump:** The DC water pump is an electronic device that pumps water using a DC motor as its main component. The DC water pump is used to pump water to the surface of the solar panel.
- **Power supply:** The power supply is a component that functions to step down or step up voltage and convert alternating current (AC) into direct current (DC). The power supply is used as the voltage source for the DC water pump.

This system setup integrates various components to monitor and optimize the solar panel's efficiency through temperature regulation.

2.2. Experimental Method

This research employed an observational methodology, wherein system performance was directly observed and recorded [19]. The study was conducted in the Renewable Energy Laboratory at Universitas Maritim Raja Ali Haji, from 09:00 to 16:00 WIB. Data was logged every 30 seconds and visualized through the ThingSpeak IoT platform to assess variations over time. Figures 1 and 2 show the study location and solar panel position.

Figure 1. Study location at Universitas Maritim Raja Ali Haji.



Figure 2. Solar panel position.



2.3. System Flowchart and Schematic Design

A flowchart illustrating the operational workflow of the device is provided in Figure 3. The system's schematic design, showing the integration of all hardware components, is shown in Figure 4.

Figure 3. System flowchart.

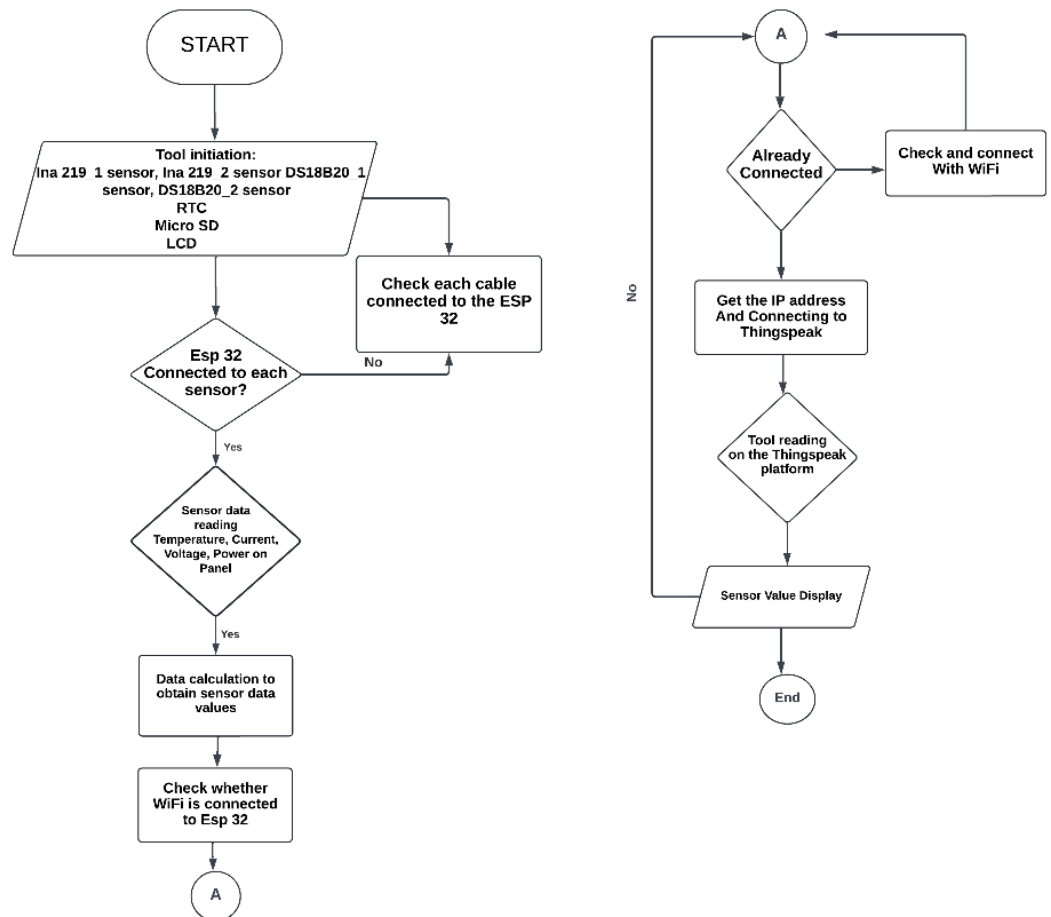
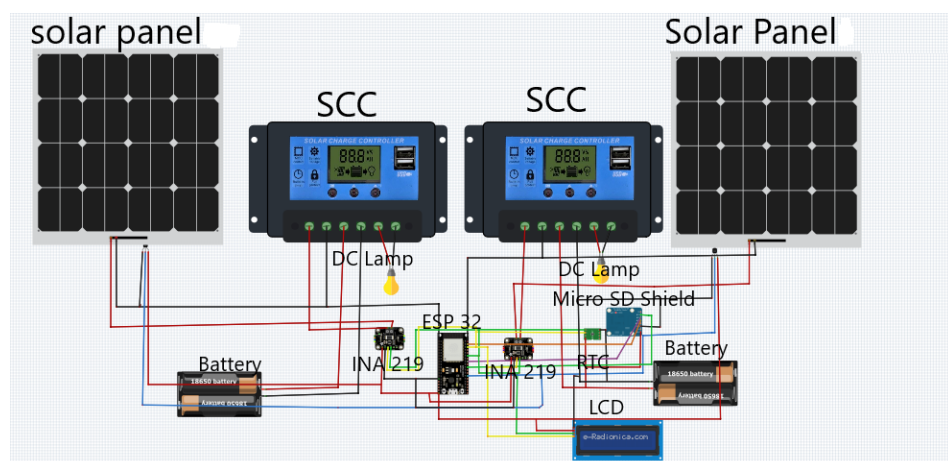


Figure 4. Schematic design of the system.



2.4. Component Testing

To validate sensor functionality, individual components were tested using calibrated instruments. The INA219 sensor was tested using a multimeter, while the DS18B20 was compared against a thermometer.

2.4.1. INA219 sensor testing

Two INA219 sensors were evaluated for accuracy by comparing their output to multimeter readings at three voltage levels: 10 V, 15 V, and 20 V. Each level was tested three times using a 100 W dummy load with 1-ohm resistance. Sensor readings were displayed via the Arduino IDE serial monitor. Error values were calculated using the following equations:

$$error = |A - Ai| \quad (1)$$

$$\%error = \frac{A - Ai}{A} \times 100\% \quad (2)$$

where A is the actual data from the measuring Instrument and Ai is the measured data from the sensor. Figure 5 shows the experimental setup for INA219 sensor testing.

Figure 5. Experimental setup for INA219 sensor testing.

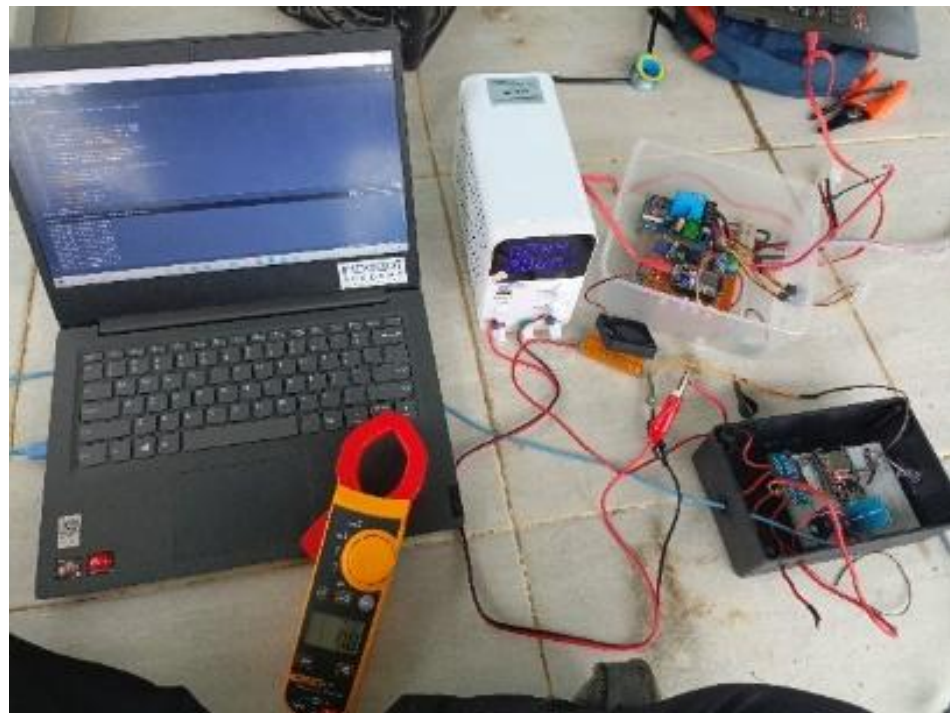


Table 1 summarizes the accuracy of the voltage and current sensors. The average error of the INA219 sensor (1) used to measure the panel with water cooling is approximately 0.11% for voltage and 0.73% for current, indicating high accuracy. The test results for the INA219 sensor (2) are shown in Table 2. The average error of sensor (2) is 0.85% for voltage and 1.26% for current.

2.4.2. DS18B20 Sensor Testing

The DS18B20 sensor was evaluated by comparing its readings to those of a thermometer. Both were attached to a heated metal rod, and the outputs were compared via the Arduino IDE serial monitor. The error was calculated using the same formulas as for the INA219 sensor. The testing process is documented in Figure 6.

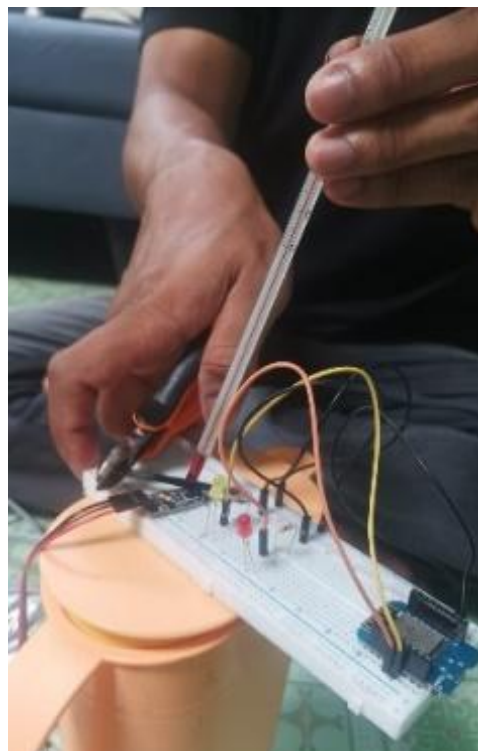
Table 1. INA219 sensor (1) testing results.

| Voltage Source | Voltage (V) | | | Current (Amp) | | |
|--------------------------|-------------|---------------|-----------|---------------|---------------|-----------|
| | Multimeter | INA219 Sensor | Error (%) | Multimeter | INA219 Sensor | Error (%) |
| 10 V | 2.1 | 2.08 | 0.95 | 2.02 | 2.02 | 0.00 |
| | 2.1 | 2.10 | 0.00 | 2.03 | 2.02 | 0.49 |
| | 2.1 | 2.10 | 0.00 | 2.03 | 2.02 | 0.49 |
| 15 V | 2.1 | 2.10 | 0.00 | 2.02 | 2.02 | 0.00 |
| | 2.1 | 2.10 | 0.00 | 2.02 | 2.02 | 0.00 |
| | 2.1 | 2.10 | 0.00 | 2.02 | 2.02 | 0.00 |
| 20 V | 2.1 | 2.10 | 0.00 | 2.00 | 2.02 | 1.00 |
| | 2.1 | 2.10 | 0.00 | 1.99 | 2.02 | 1.51 |
| | 2.1 | 2.10 | 0.00 | 1.96 | 2.02 | 3.06 |
| Average Error Percentage | | | 0.11 | 0.73 | | |

Table 2. INA219 sensor (2) testing results.

| Voltage Source | Voltage (V) | | | Current (Amp) | | |
|--------------------------|-------------|---------------|-----------|---------------|---------------|-----------|
| | Multimeter | INA219 Sensor | Error (%) | Multimeter | INA219 Sensor | Error (%) |
| 10 V | 2.1 | 2.08 | 0.95 | 2.08 | 2.02 | 2.88 |
| | 2.1 | 2.09 | 0.48 | 2.04 | 2.02 | 0.98 |
| | 2.1 | 2.09 | 0.48 | 2.04 | 2.02 | 0.98 |
| 15 V | 2.1 | 2.08 | 0.95 | 1.96 | 2.02 | 3.06 |
| | 2.1 | 2.08 | 0.95 | 2.05 | 2.02 | 1.46 |
| | 2.1 | 2.08 | 0.95 | 2.00 | 2.02 | 1.00 |
| 20 V | 2.1 | 2.08 | 0.95 | 2.02 | 2.02 | 0.00 |
| | 2.1 | 2.08 | 0.95 | 2.03 | 2.02 | 0.49 |
| | 2.1 | 2.08 | 0.95 | 2.03 | 2.02 | 0.49 |
| Average Error Percentage | | | 0.85 | 1.26 | | |

Figure 6. Testing process of DS18B20 sensor.



The accuracy of the DS18B20 temperature sensor (1) is summarized in Table 3, where the average error is 0.54°C, and the percentage error is 1.23%. The DS18B20 sensor (2) shows an average error of 0.64°C and a percentage error of 1.46% as shown in Table 4.

Table 3. Temperature accuracy of DS18B20 sensor (1).

| Thermometer Measurement (°C) | DS18B20 Measurement (°C) | Error (%) |
|---------------------------------|-----------------------------|-----------|
| 50 | 49.44 | 1.12 |
| 49 | 48.61 | 0.80 |
| 48 | 47.75 | 0.52 |
| 47 | 46.79 | 0.45 |
| 46 | 45.55 | 0.98 |
| 45 | 44.70 | 0.67 |
| 44 | 43.25 | 1.70 |
| 43 | 42.12 | 2.05 |
| 42 | 41.22 | 1.86 |
| 41 | 40.17 | 2.02 |
| 40 | 39.44 | 1.40 |
| Average Error Percentage | | 1.23 |

Table 4. Temperature accuracy of DS18B20 sensor (2).

| Thermometer Measurement (°C) | DS18B20 Measurement (°C) | Error (%) |
|---------------------------------|-----------------------------|-----------|
| 50 | 49.44 | 1.12 |
| 49 | 48.61 | 0.80 |
| 48 | 47.75 | 0.52 |
| 47 | 46.79 | 0.45 |
| 46 | 45.55 | 0.98 |
| 45 | 44.70 | 0.67 |
| 44 | 43.25 | 1.70 |
| 43 | 42.12 | 2.05 |
| 42 | 41.22 | 1.86 |
| 41 | 40.17 | 2.02 |
| 40 | 39.44 | 1.40 |
| Average Error Percentage | | 1.23 |

3. Results and Discussion

The physical appearance of the device is shown in Figure 7, with the internal view depicted in Figure 8. The web dashboard displayed on the ThingSpeak platform is provided in Figure 9.

Figure 7. Physical appearance of the device.



Figure 8. Components inside the device.

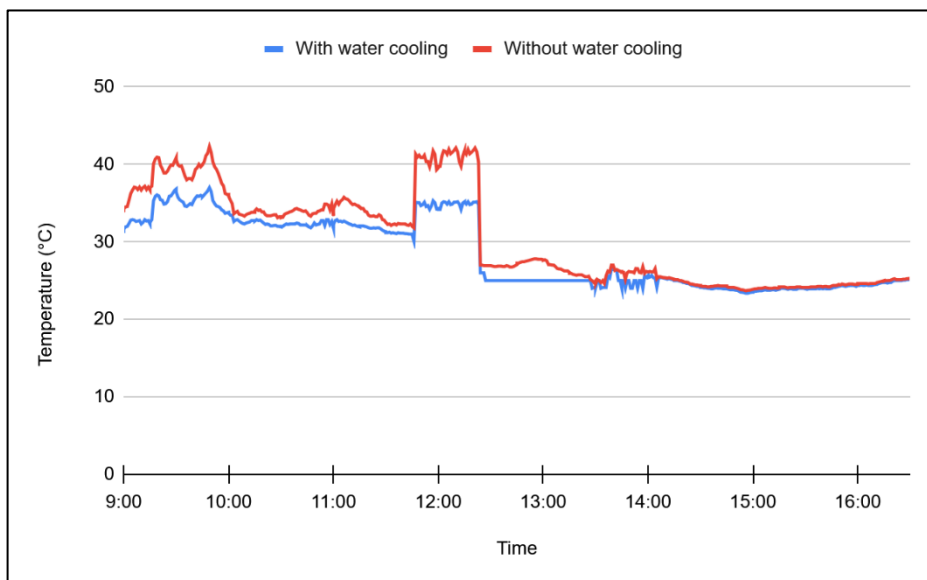


Figure 9. ThingSpeak dashboard web interface.

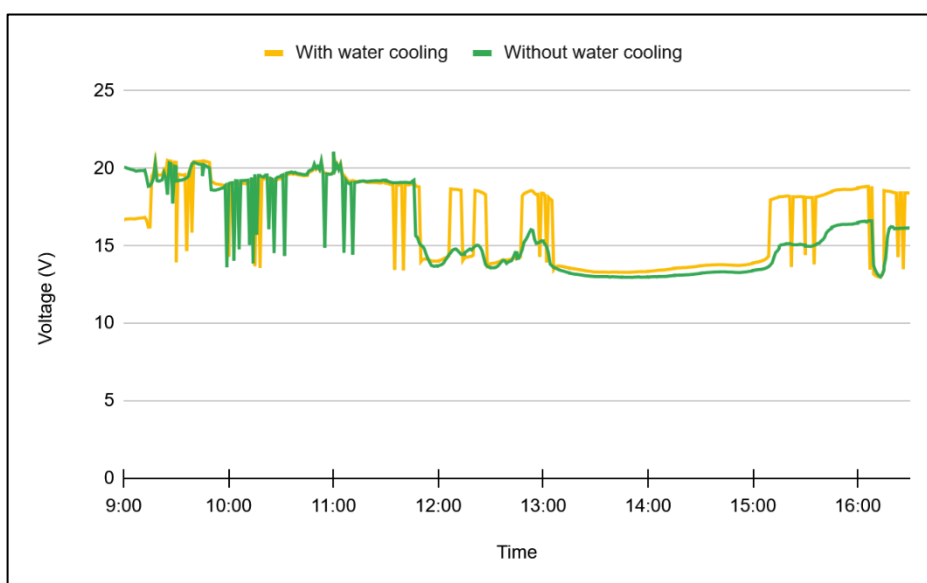


The temperature, voltage, and current data for the first day of testing are shown in Figure 10. On the first day, clear trends were observed in the performance of both panels. The water-cooled panel maintained a lower average temperature of 28.5°C, while the non-cooled panel averaged 30.3°C, indicating a 1.8°C reduction due to water cooling. This reduction aligns with previous findings that lower operating temperatures lead to improved photovoltaic efficiency. The voltage output of the panels supports this trend. The cooled panel delivered an average voltage of 16.7 V, compared to 16.04 V for the non-cooled panel — a difference of 0.66 V. This voltage gain represents a significant improvement in power output, especially when scaled across large installations. Although the current difference was minimal due to the regulation by the Solar Charge Controller (SCC), which only increases current flow when the battery requires charging, it still affirms the primary finding that temperature has a direct influence on panel voltage output.

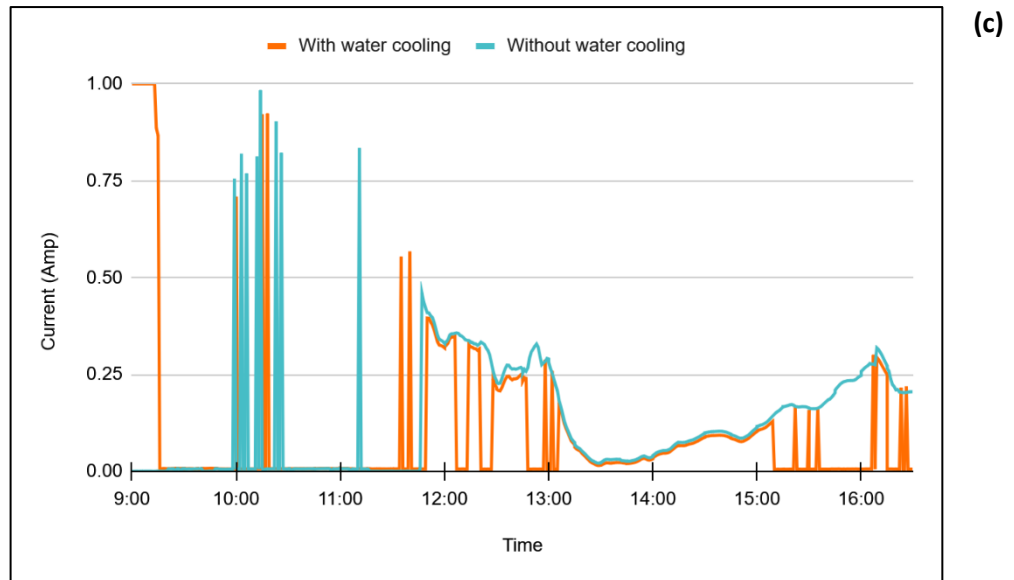
Figure 10. Comparison of solar panel with water cooling vs without water cooling on day 1: **(a)** temperature, **(b)** output voltage, **(c)** output current.



(a)

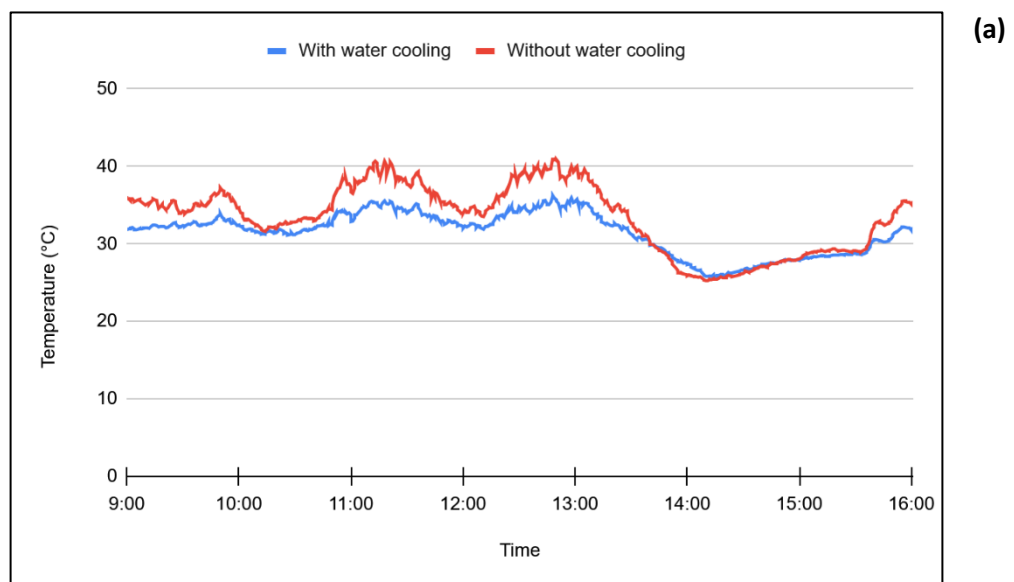


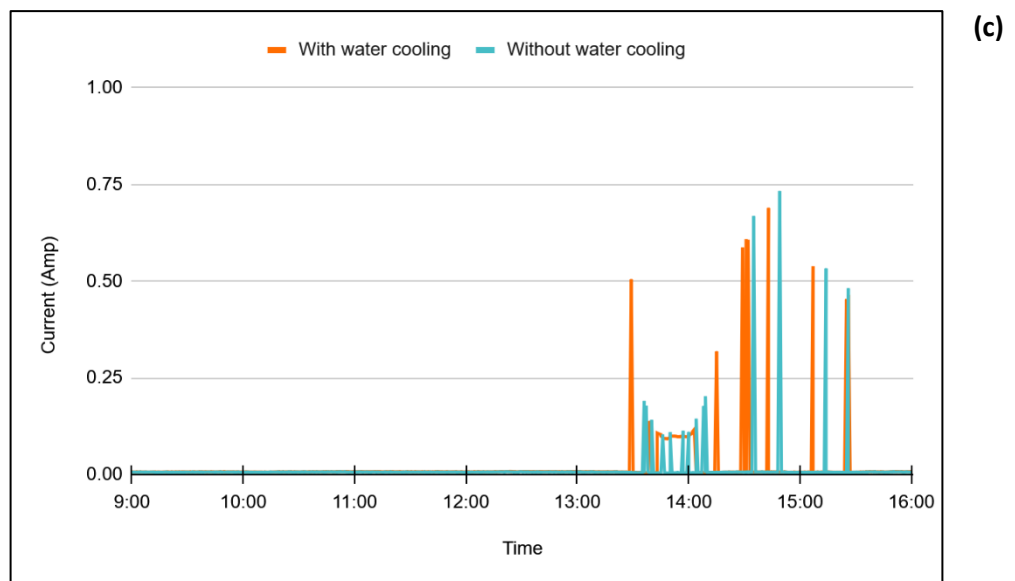
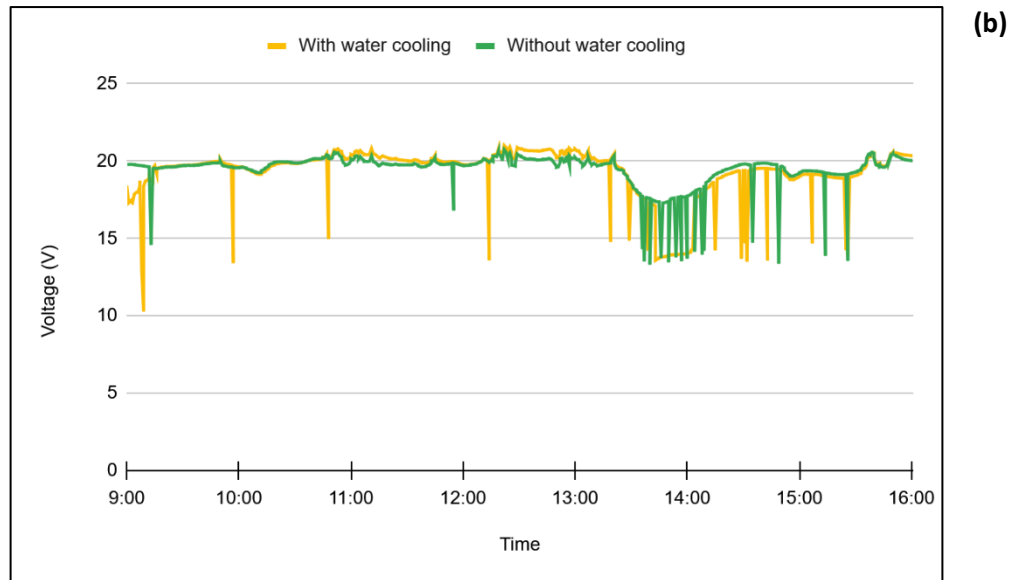
(b)



The second day followed a similar pattern but with slightly higher temperatures overall. The water-cooled panel reached an average temperature of 31.4°C, while the non-cooled panel rose to 33.4°C, maintaining the ~2°C cooling benefit. Interestingly, the voltage results showed the opposite trend: the non-cooled panel produced a slightly higher average voltage of 19.46 V compared to 19.27 V from the cooled panel. This anomaly may be attributed to external environmental variables such as cloud cover, irradiance angle, or temporary shading, which were not directly measured in this study. Despite this, the temperature difference remained consistent, suggesting that the cooling system functioned reliably, even if its voltage advantage was offset by other factors on that day. The current output increased noticeably in the afternoon (13:00 to 16:00), likely because the battery reached a lower charge threshold, prompting the SCC to draw more current. This illustrates the dynamic nature of current regulation and the importance of considering system demand in evaluating panel performance. The results of the second day experiment are shown in Figure 11.

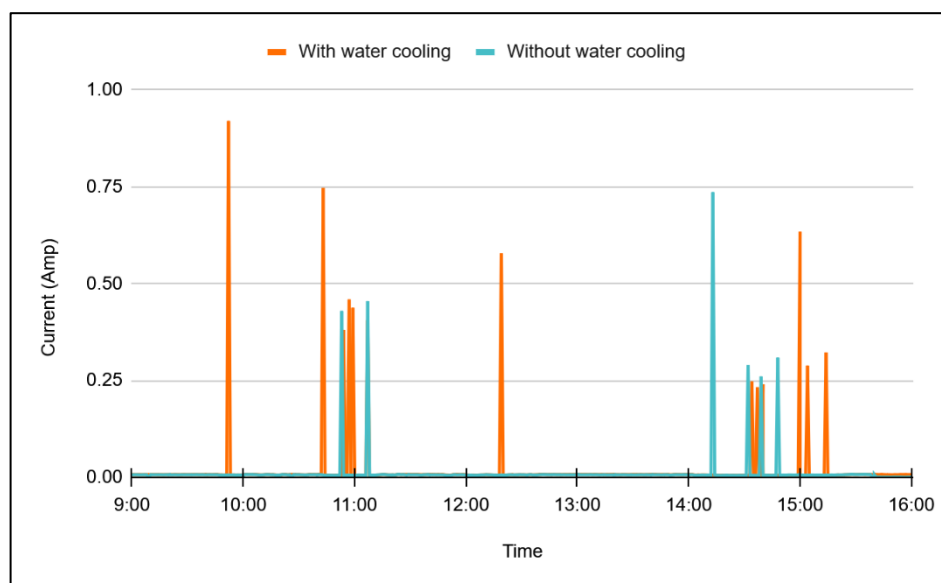
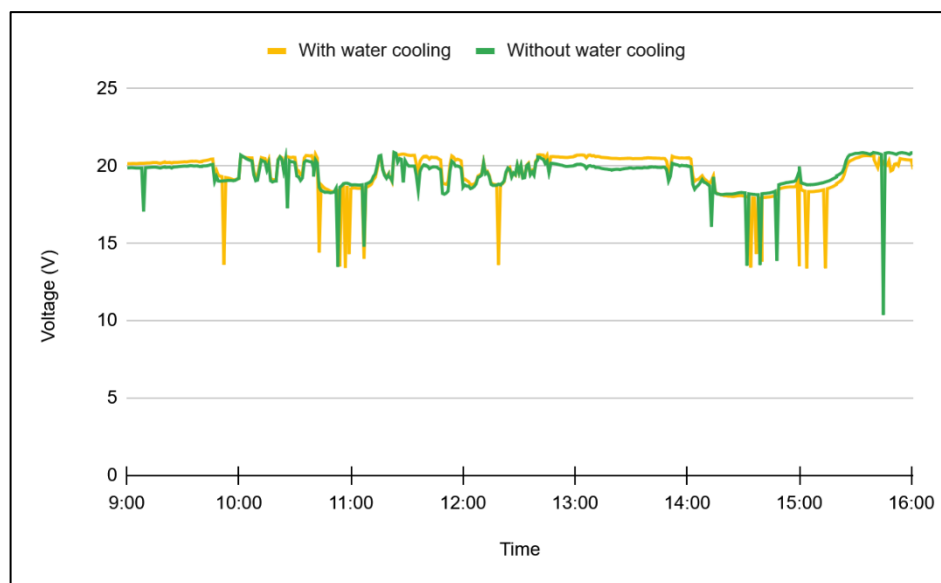
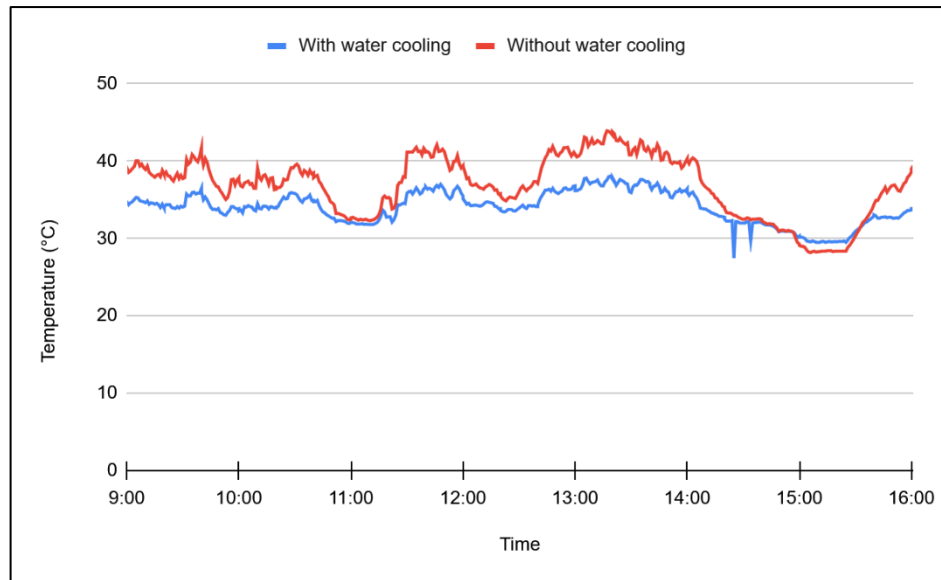
Figure 11. Comparison of solar panel with water cooling vs without water cooling on day 2: **(a)** temperature, **(b)** output voltage, **(c)** output current.





Day 3 recorded the highest temperature readings across the study. The water-cooled panel had an average temperature of 34.0°C, while the non-cooled panel reached 36.8°C, maintaining a cooling effect of nearly 3°C — the greatest temperature reduction observed across all three days. In terms of voltage, the cooled panel again performed better, averaging 19.58 V versus 19.49 V for the non-cooled panel. While this difference is modest (0.09 V), it reaffirms that even small temperature reductions can have a measurable impact on output voltage, particularly under high-irradiance conditions. The current readings were more erratic on Day 3 due to changes in the type and condition of the batteries used. This variability complicated direct comparison, but it emphasizes the need for consistent system configurations when conducting such studies. The results can be seen in Figure 12.

Figure 12. Comparison of solar panel with water cooling vs without water cooling on day 3: **(a)** temperature, **(b)** output voltage, **(c)** output current.



Across all three days, the cooling system consistently reduced the operating temperature of the solar panels. The voltage performance generally correlated with temperature, confirming the hypothesis that thermal regulation can enhance photovoltaic efficiency. The marginal gains in voltage (0.09–0.66 V), though small in absolute terms, become meaningful in scalable solar arrays, where even fractional improvements can translate to significant energy and cost savings. Additionally, the real-time monitoring enabled by the IoT system proved essential for capturing and analyzing these trends.

4. Conclusion

This study, which involved the design, component testing, implementation, and analysis of an IoT-based monitoring system, led to several key conclusions. The system functioned as expected, effectively evaluating the impact of water flow on solar panel efficiency. Panels with water circulation maintained lower operating temperatures and produced higher average voltage outputs compared to those without cooling. This finding reaffirms the critical role of temperature in photovoltaic efficiency. While current measurements were not included due to the configuration of the Solar Charge Controller (SCC), the system successfully facilitated real-time monitoring and data acquisition.

The water-cooling approach demonstrated significant potential for practical application, especially in regions with high solar irradiance where temperature regulation is essential for optimizing energy production. Its simplicity and low operational cost make it an ideal solution for small to medium-scale solar installations. Furthermore, with appropriate modifications, this cooling system could be scaled for larger setups. Future research should focus on assessing the long-term effectiveness of this cooling method under varied environmental conditions, evaluating water resource efficiency, and exploring the comparison between passive and active cooling strategies. These studies would provide valuable insights into further optimizing solar energy systems for enhanced performance and sustainability.

Funding: This research received no external funding.

Data Availability Statement: “The data that support the findings of this study are available from the corresponding author upon reasonable request.”

Conflicts of Interest: The authors declare no conflicts of interest.

References

- [1] S. Wang *et al.*, “Anti-reflection effect of high refractive index polyurethane with different light trapping structures on solar cells,” *Heliyon*, vol. 9, no. 9, p. e20264, Sep. 2023, doi: 10.1016/j.heliyon.2023.e20264.
- [2] M. S. Sheik, P. Kakati, D. Dandotiya, U. R. M, and R. C. S, “A comprehensive review on various cooling techniques to decrease an operating temperature of solar photovoltaic panels,” *Energy Nexus*, vol. 8, p. 100161, Dec. 2022, doi: 10.1016/j.nexus.2022.100161.
- [3] R. Salehi, A. Jahanbakhshi, M. Reza Golzarian, and M. Khojastehpour, “Evaluation of solar panel cooling systems using anodized heat sink equipped with thermoelectric module through the parameters of temperature, power and efficiency,” *Energy Conversion and Management: X*, vol. 11, p. 100102, Sep. 2021, doi: 10.1016/j.ecmx.2021.100102.
- [4] S. Dhanalakshmi *et al.*, “Thermal management of solar photovoltaic panels using a fibre Bragg grating sensor-based temperature monitoring,” *Case Studies in Thermal Engineering*, vol. 31, p. 101834, Mar. 2022, doi: 10.1016/j.csite.2022.101834.
- [5] G. R. Cahyono, P. R. Ansyah, and N. Q. Awaly, “Pendinginan panel surya menggunakan kotak pendingin dan sirip pendingin,” *Angkasa: Jurnal Ilmiah Bidang Teknologi*, vol. 13, no. 1, pp. 73–79, May 2021, doi: 10.28989/angkasa.v13i1.947.

- [6] Z. Xu, Q. Kong, H. Qu, and C. Wang, "Cooling characteristics of solar photovoltaic panels based on phase change materials," *Case Studies in Thermal Engineering*, vol. 41, p. 102667, Jan. 2023, doi: 10.1016/j.csite.2022.102667.
- [7] S. M. Shalaby, M. K. Elfakharany, B. M. Moharram, and H. F. Abosheisha, "Experimental study on the performance of PV with water cooling," *Energy Reports*, vol. 8, pp. 957–961, Apr. 2022, doi: 10.1016/j.egy.2021.11.155.
- [8] R. Salehi, A. Jahanbakhshi, J. B. Ooi, A. Rohani, and M. R. Golzarian, "Study on the performance of solar cells cooled with heatsink and nanofluid added with aluminum nanoparticle," *International Journal of Thermofluids*, vol. 20, p. 100445, Nov. 2023, doi: 10.1016/j.ijft.2023.100445.
- [9] L. Chanphavong, V. Chanthaboune, S. Phommachanh, X. Vilaida, and P. Bounyanite, "Enhancement of performance and exergy analysis of a water-cooling solar photovoltaic panel," *Total Environment Research Themes*, vol. 3–4, p. 100018, Dec. 2022, doi: 10.1016/j.totert.2022.100018.
- [10] T. Azad, M. A. H. Newton, J. Trevathan, and A. Sattar, "IoT edge network interoperability," *Comput Commun*, vol. 236, p. 108125, Apr. 2025, doi: 10.1016/j.comcom.2025.108125.
- [11] M. J. Mnati, R. F. Chisab, A. M. Al-Rawi, A. H. Ali, and A. Van den Bossche, "An open-source non-contact thermometer using low-cost electronic components," *HardwareX*, vol. 9, p. e00183, Apr. 2021, doi: 10.1016/j.ohx.2021.e00183.
- [12] M. Melvi, A. Ulvan, M. R. Sidiq, and M. A. M. Batubara, "Rancang Bangun Sistem Monitoring Ketinggian Muka Air Laut Menggunakan Arduino Pro Mini dan NodeMCU ESP8266," *Jurnal Teknologi Riset Terapan*, vol. 1, no. 1, pp. 25–35, Feb. 2023, doi: 10.35912/jatra.v1i1.1794.
- [13] Tito Ahmad Fauzan, Rahman Arifuddin, and Resi Dwi Jayanti Kartika Sari, "Sistem Manajemen Baterai Pada Peralatan Catu Daya Di Equipment Room Stasiun Manggarai Dengan Aplikasi Blynk Berbasis Esp8266," *Uranus: Jurnal Ilmiah Teknik Elektro, Sains dan Informatika*, vol. 2, no. 3, pp. 174–195, Jul. 2024, doi: 10.61132/uranus.v2i3.270.
- [14] B. J. Setiawan, "Design and Build Voltage and Current Monitoring Parameters Device of Rechargeable Batteries in Real-Time Using the INA219 GY-219 Sensor," *Journal of Energy, Material, and Instrumentation Technology*, vol. 4, no. 2, pp. 58–71, May 2023, doi: 10.23960/jemite.v4i2.137.
- [15] M. Baehaqi, A. Rosyid, A. Siswanto, and E. Subiyanta, "Performance Testing of DHT11 and DS18B20 Sensors as Server Room Temperature Sensors," *Mestro: Jurnal Teknik Mesin Dan Elektro*, vol. 5, no. 2, pp. 6–11, 2023.
- [16] D. Yulizar, S. Soekirno, N. Ananda, M. A. Prabowo, I. F. P. Perdana, and D. Aofany, "Performance Analysis Comparison of DHT11, DHT22 and DS18B20 as Temperature Measurement," 2023, pp. 37–45. doi: 10.2991/978-94-6463-232-3_5.
- [17] Arief Goeritno, Muhammad Azril Maulana, Fauzan Shulhan, and Hakim Fiqwananda, "Pemasangan Solar Panel Untuk Sistem Charging Power Station di Kawasan Ekowisata Gunung Kuta, Kabupaten Bogor," *Mitra Teras: Jurnal Terapan Pengabdian Masyarakat*, vol. 2, no. 2, pp. 42–57, Dec. 2023, doi: 10.58797/teras.0202.04.
- [18] S. Yuwono, D. Diharto, and N. W. Pratama, "Manfaat Pengadaan Panel Surya dengan Menggunakan Metode On Grid," *Energi & Kelistrikan*, vol. 13, no. 2, pp. 161–171, Dec. 2021, doi: 10.33322/energi.v13i2.1537.
- [19] Mhd. P. Hasibuan, R. Azmi, D. B. Arjuna, and S. U. Rahayu, "Analisis Pengukuran Temperatur Udara dengan Metode Observasi," *Jurnal Garuda Pengabdian Kepada Masyarakat*, vol. 1, no. 1, pp. 8–15, 2023.

Disclaimer/Publisher's Note: The statements, opinions and data contained in all publications are solely those of the individual author(s) and contributor(s) and not of MSD Institute and/or the editor(s). MSD Institute and/or the editor(s) disclaim responsibility for any injury to people or property resulting from any ideas, methods, instructions or products referred to in the content.